Journal of Applied Sciences and Emerging Technologies Vol. 1, Issue 1, 2023

Flow Induced Vibration Analysis of Grooved Cylinder in Heat Exchanger

Javaria Qadeer [1*], Riffat Asim Pasha [1], Muhammad Moin Akhtar [1], Muhammad Ammar Akram [2], Hassan Shehwar Shah [1], and Bushra Nadeem [1]

[1] Department of Electrical Engineering, University of Engineering and Technology (UET), Taxila, Pakistan.
[2]HITEC University Taxila Cantt., Taxila, Pakistan.

* Correspondence: javariaqadeer.a@gmail.com;

Received date: 04-03-2023
Accepted date: 05-15-2023
Published date: 19-07-2023

Abstract: For enhancing the performance of Shell and Tube Heat Exchanger the impact of establishing a square groove along the length of a shell and tube heat exchanger is investigated experimentally. Therefore, an experimental investigation is conducted for turbulent cross-flow in a parallel triangular tube bundle with pitch to diameter P/D ratio of 1.45. The 300mm long cylinder is patterned with square grooves extending longitudinally. Tube bundles consist of 50 tubes with an average diameter of 12mm. Tubes are placed in a staggered pattern. There are two grooves, at 90° and 270°, on the outside of cylinder. These experiments are carried out in a wind tunnel that operates at subsonic speeds. The monitored tube response appears to be strongly influenced by its position inside a particular row in both the stream-wise and transverse directions. Additionally, the third row plays a significant role in the early stability of the tube being monitored specifically in the transverse direction.

Keywords: Instability, Parallel Triangular, STHE, Tube bundle.

1. Introduction

Heat exchangers are an essential component of many mechanical systems and have numerous applications in a diverse range of industries as well as power plants. Heat exchangers come in a wide variety of shapes and sizes, each designed for a particular set of

situations. There are several reasons for the significance of Shell and Tube Heat Exchangers (STHEs). Flow-induced vibration has essential technological applications in sectors such as aircraft wings, nuclear fuel bundles, centrifugal pumps as well as power transmission lines in addition to its apparent importance in shell-and-tube heat exchangers. Therefore, specialists in this subject investigate the responses of elastic structures to fluid motion [1]. In the past, components were constructed with high safety factors, resulting in constructions that were robust and long-lasting. Constant attention was paid to the potential for flow-induced vibration while developing these buildings. When lighter components, flexible structures, and greater flow velocities were progressively used to boost performance, problems originating from flow-induced vibrations started to emerge. Therefore, it became clear that flow-induced vibration is an issue that must be taken into account throughout the design process [2].

Numerous real-world applications have prompted extensive study of flow around a circular cylinder, including towers, offshore projects, and heat exchangers. The literature has several studies of both laminar and turbulent flow regimes in circular cylinders [3]. A laminar viscous flow can change into a number of other flow regimes at low Reynolds numbers. $Re = UD/\vartheta$ is the formula for calculating Reynolds number, where U denotes the fluid's free-stream velocity, D is cylinder's hydraulic diameter, which is the same as its diameter, and v is the kinematic viscosity of the fluid. Despite having the appearance of the most straightforward cross-section geometry, a circular cylinder's wake structure depends on several variables such as cylinder’s aspect ratio, roughness of surface, as well as the blockage ratio. It has been shown that the wake of a cylinder is considerably impacted by the surface roughness [4]. Dimples, longitudinal grooves, or ridges on the surface of a cylinder may be used to evaluate its roughness in comparison to a smooth cylinder. The instabilities in flow regime, Von Karman Street (VKS) and the wake structure are all brought about by the creation of surface roughness via any of the methods listed above [5].

Using wind tunnel studies, Bearman and Harvey discovered that the critical regime occurs at a lower Re for a dimpled circular cylinder than for a plain circular cylinder. Furthermore, it was presented that at a Reynolds number of $Re = 10^5$, the dimples of the cylinder can lower drag forces by as much as 50% when compared to smooth cylinders. Bearman and Harvey found that the Strouhal Number ($St = fD/U$) for a dimpled cylinder is equal to smooth circular cylinder when $Re < 4 \times 10^4$ [6]. By increasing Re to 10^5 help Strouhal number to approach to its maximum $St = 0.32$. The experiments provided strong evidence for the effect of dimpled surfaces on reducing drag force, the arrangement of the

grooves as well as the geometry of the dimples were not taken into consideration in this research [7].

The majority of study has focused on FEI (Fluid Elastic Instability) effect of tube bundle in circular cylinders, but several noteworthy investigations have been conducted on the basis of modified tube shape assertions. Lam et al. noted that a wavy surfaced cylinder might weaken, thus decreasing the vibration, when compared to a circular cylinder at the same Reynolds numbers [8]. In the literature, bluff bodies with multiple grooves are employed, with the exception of the work by Kimura and Tsutahara (1990), who report reduced drag around a circular cylinder with a single groove of varying diameters at subcritical Reynolds numbers. It has also been found that the size of the grooves plays a different role than the surface roughness in regulating the flow separation [9]. When the length of the groove is increased, the separation point shifts to the leading edge of grooves [10]. Quantitative dye experiments as well as two-dimensional numerical simulations are both part of their research. The effect of longitudinally pattern groove on the wake of circular cylinder was recently investigated by Canpolat (2015) through comprehensive observations. Within the solid body, a single groove on a spherical body distributes periodic loadings more evenly, production time and costs are reduced while endurance is improved due to lower stress concentration [11]. According to Parnaudeau et al. (2008), the subcritical flow regime is commonly used in industry and can be easily observed. Therefore, significant information regarding the wake of a circular cylinder at the present flow circumstances ($Re = 5000$) can significantly advance the relevant literature. In this study, we use the boundary layer thickness of a circular cylinder as a measurement for defining groove size. This information comes from the work of Willmarth et al (1976). To cause disturbances in the boundary layer, dimensions of w×h=5mm×5mm have been employed.

In this research work, three design factors were investigated: the depth of the grooves at constant width, the number of grooves (more specifically, the area of the cylinder occupied by grooves), and the shape of the grooves (that is, circular versus square section). With low Reynolds numbers, this research aims to maximize groove width and geometry for drag reduction performance. The objective of this research is to conduct an experimental investigation of how grooves affect flow in a parallel triangular configuration of tube bundle.

2. Materials and Methods

Experiments in a GUNT low-speed open-loop wind tunnel (model HM 170) is performed. The test section has an internal cross-section area of (300x300) mm and is made

up of acrylic plates. The studied model is mounted in the test section and the flow medium (air) is set to move as to achieve the desired flow in the wind tunnel. The precisely designed flow straightener and nozzle contour in the wind tunnel make sure a uniform velocity distribution with a turbulence level less than 1 % of the test section. The built-in variable speed drive and axial fan with downstream guide vanes make sure an energy-efficient operation at maximum efficiency. An airflow velocity of 0 to 28 m/s in this open-loop wind tunnel is achieved when no test model being placed within 0.7 to 8.2 m/s. To measure the flow velocity of air, a manometer is placed at 150 mm upstream of the tube bundle. This manometer is connected with a digital differential pressure transducer to display the flow velocity. An uncertainty of ±0.025 m/s in the measurement of flow velocity is possible. HM 170 system for data acquisition is used. The measured values of velocities by this system can be transferred to a computer and saved as an Excel file. Line diagram of the Subsonic wind tunnel which is used in experimentation is shown in Figure 1(a). Figure 1(c) shows the geometry of the grooved tube that was used in experiments having length of 300 mm and diameter of 12 mm, while the width and depth of the groove is 3 mm. Experiments on parallel triangular tube bundle arrangement with a pitch to diameter ratio P/D of 1.45 is performed.

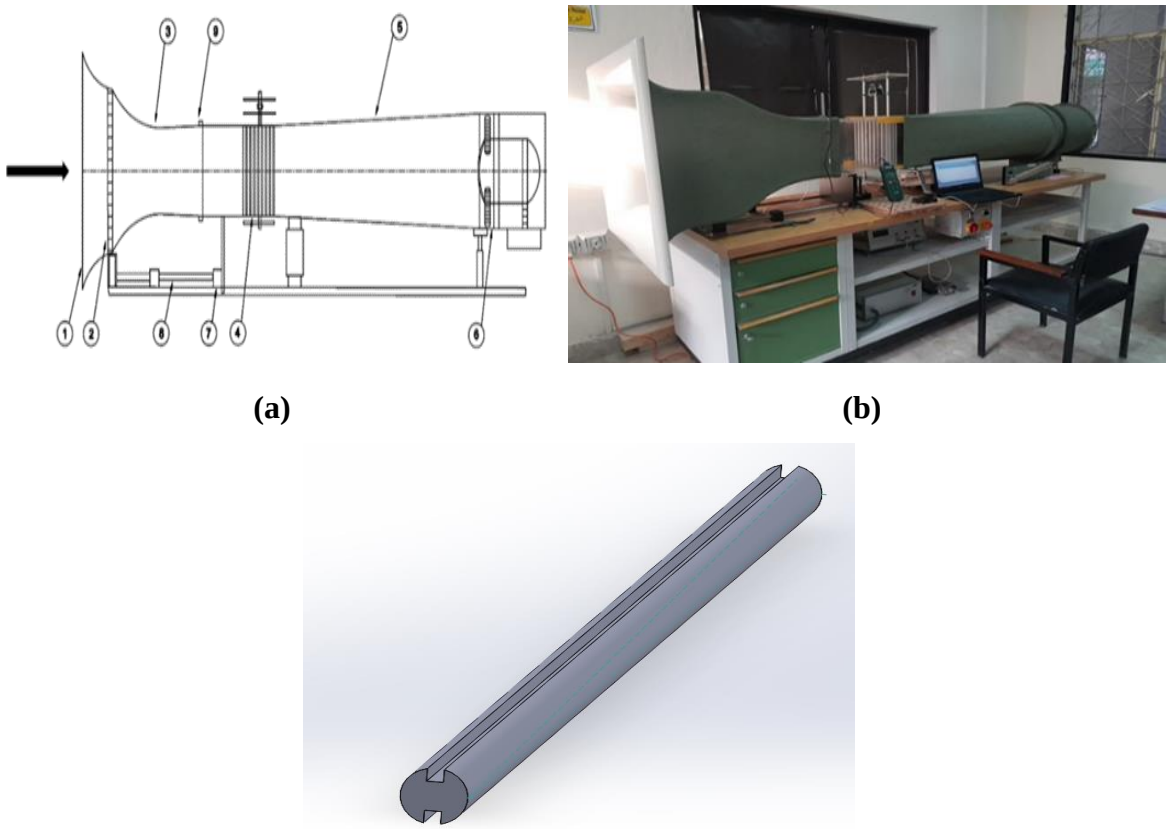

(a) **(b)**

(c)

Figure 1: (a) Line diagram (b) an image of an experimental wind tunnel setup with its many parts identified as follows: (1) funnel; (2) flow straightener; (3) converging section;

(4) test model (5) Diverging section (6) Axial fan; (7) Tunnel pillar (8) a length gauge with a variable scale; (9) velocity measuring probes (c) Geometry of grooved tube

There were 5 rows and 10 columns of tubes. A total of 50 Aluminum tubes, having one central flexible tube instrumented with a tri-axial accelerometer. Experiments were performed in the first three rows. For each row, a central flexible tube was monitored by the tri-axial accelerometer. Experimentations started with a flow velocity of 2.2 m/s, then we increased flow velocity by the difference of 0.5 m/s. At each flow velocity, we gave 10 seconds to the accelerometer to capture the vibration response of the tube. The vibration response of the tube from a flow velocity of 2.2 m/s to 8.2 m/s is captured. The complete specifications of the tube bundle are shown in table 1.

Table 1: Specifications of the tube bundle

Tube bundle configuration	**Parallel Triangular arrangement**
Total number of tubes	50
Tube’s material	Aluminum
Length of tube	300 mm
Pitch to diameter ration P/D	1.45
Outer diameter of tubes	12mm
Tube’s mass/unit length	0.330 kg/m
Tube’s modulus of elasticity	69000 MPa
Density of air	1.225 kg/m^3
Density of tube	2800 kg/m^3

The measured tube was hung from a piano wire that measured 0.2 mm in diameter. Furthermore, a tensioning device was included for fine-tuning the wire's tension. First-, second-, and third-row tubes' natural frequencies were set to 14, 14, and 11.8 Hz, respectively, with a 0.5% margin of error. For recording the tube’s vibrations accelerometer was used. It was placed at the top of the flexible tube and then the vibration response was monitored and recorded on the PC. 4 number of acrylic plates were used for holding the tube bundles together. Two of these plates held the stiff tubes and two of which held the tension mechanism. Parts of the tube bundle and how they fit together are seen in Figure 2.

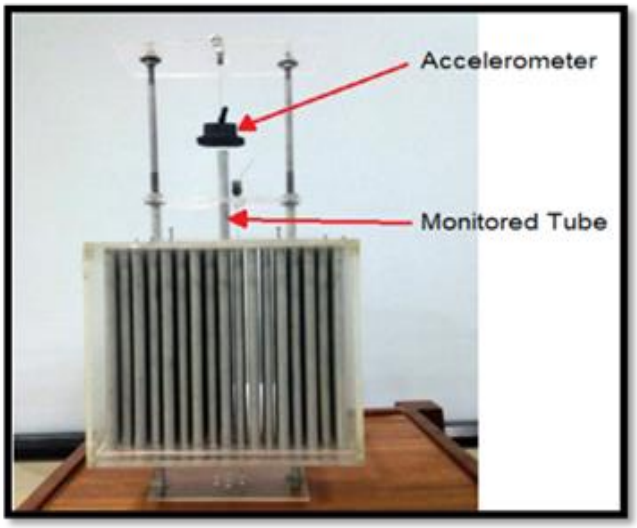

Figure 2: Tube Bundle

In order to record the tube's vibration response, a data gathering system is employed comprised of a G-link wireless tri-axial accelerometer sensor node, a WSDA wireless USB base station, and a PC running Microstrain Corporation's Node Commander software. A sampling frequency of 376 Hz was to obtain data. To obtain good repeatability of the results the signal from each sensor was averaged and obtained data saved in an Excel file for further analysis. The data was imported to Origin Pro software developed by Origin Lab Corporation for obtaining the time domain and frequency domain signals of vibration response. First of all, time waveforms were obtained then Fast Fourier Transformation applied to get frequency spectrum of respective time waveform. All-time waveforms and frequency spectrums were analyzed. It was difficult to interpret results from time waveforms, that’s why signals were imported into Sig-view software to get room mean square values for each time waveform.

3. Results

The instability of single flexible tubes in a rigid array was found to be highly location dependent through a series of experiments conducted on bare tubes. Many scientists have used and supported this concept. There are a large number of empirical coefficients that must be determined in order to fully understand the complexity of a fully flexible tube array. This method simplifies the problem so that we can gain a deeper understanding of the underlying physics of the observed phenomenon. The fluid-elastic instability threshold for both the single flexible as well as the fully flexible tubes in a tube bundle is same so about same of the configurations can be applied for the single flexible tube like that of the fully flexible tubes in a tube bundle.

Natural frequency of single flexible tube was obtained by using the pluck method. Tube is initially excited and then set for free vibrations. Then the frequency of the free vibrations

is measured that is basically the tube's natural frequency. The monitored tube's natural frequency was observed nearly at 10Hz. Here, translational and rocking mode of tube was observed.

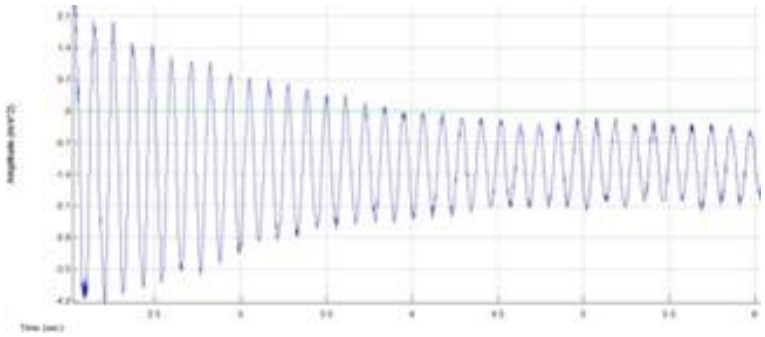

Figure 3: Vibration Response of Tube

Spectral analysis of the monitored grooved tube is shown in Fig 4. Time as well as the frequency domains for 2nd, 3rd and 4th row of the heat exchanger tube bundles with parallel triangular arrangement and pitch to diameter ratio of 1.45 are plotted. Two velocity values are considered for analyzing the results that are 3.7 m/s and 8.2 m/s. Time spectrum shows the vibrations of the monitored tube with respect to time. The data is analyzed up to 6500 seconds. Frequency spectrum shows the tube's amplitude with the passage of time as the velocity of the flow changes.

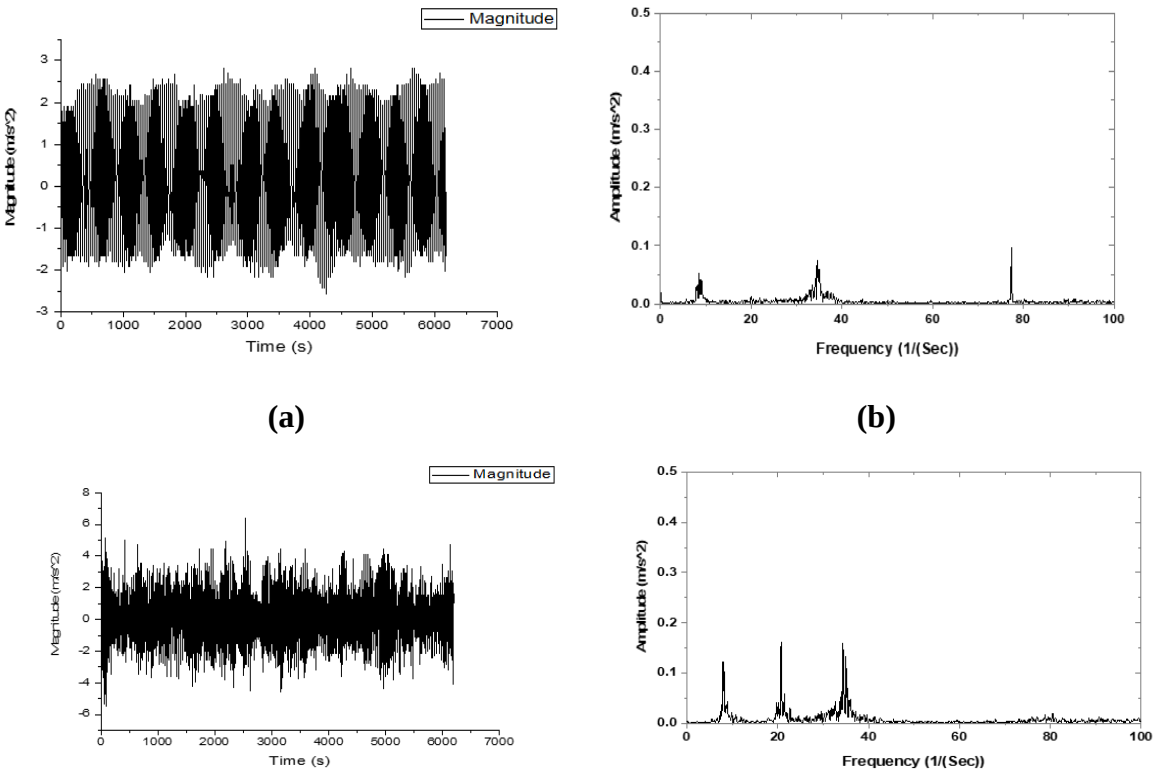

(c)

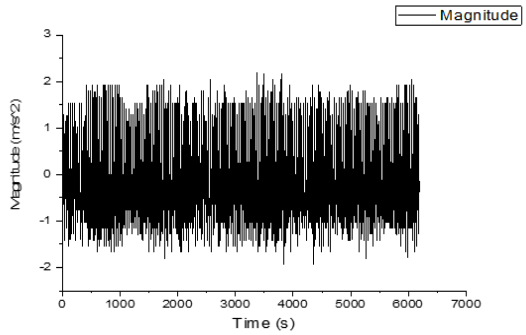
Magnitude
Magnitude (m/s^2)
Time (s)

(d)

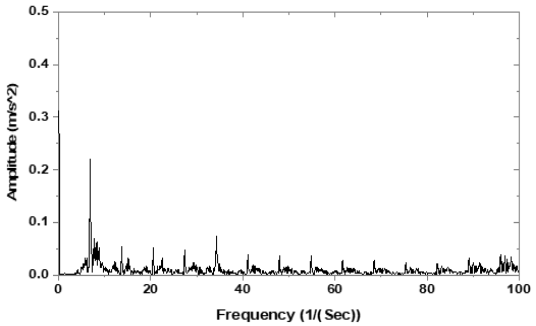
Amplitude (m/s^2)
Frequency (1/(Sec))

(e)

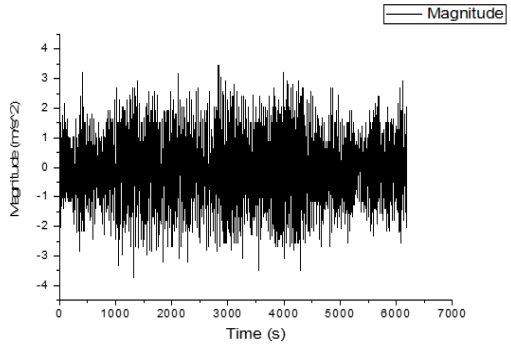
Magnitude
Magnitude (m/s^2)
Time (s)

(f)

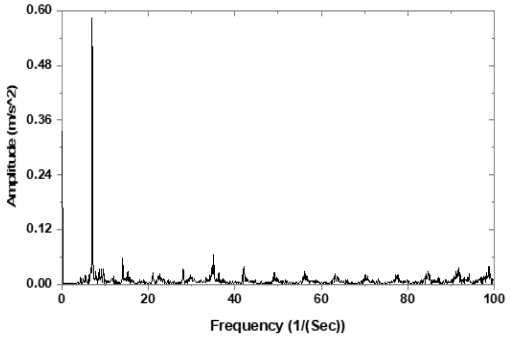
Amplitude (m/s^2)
Frequency (1/(Sec))

(g)

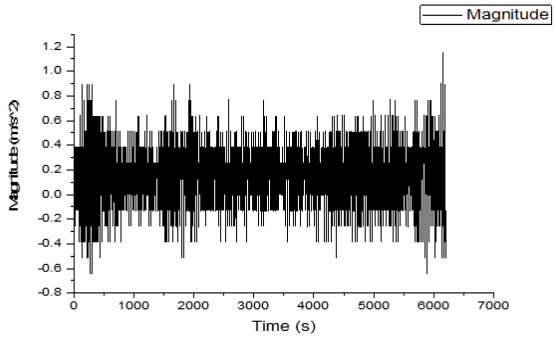
Magnitude
Magnitude (m/s^2)
Time (s)

(h)

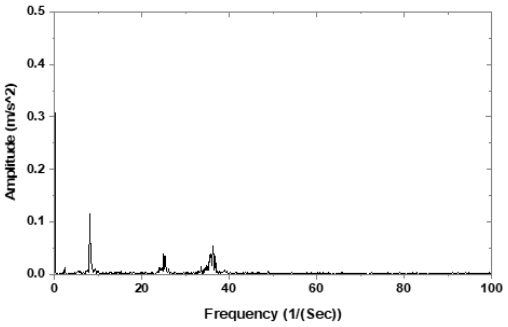
Amplitude (m/s^2)
Frequency (1/(Sec))

(i)

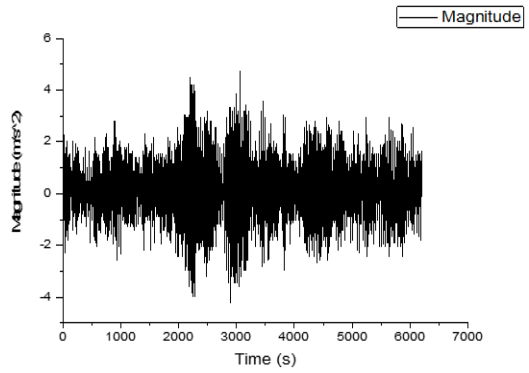
Magnitude
Magnitude (m/s^2)
Time (s)

(j)

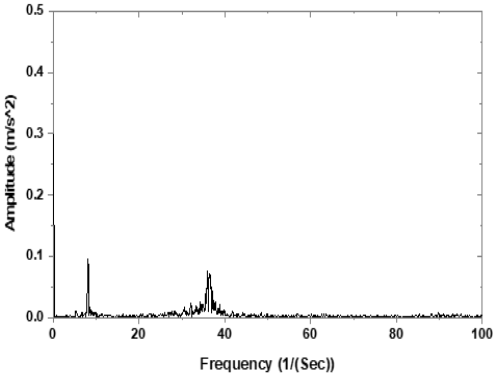
Amplitude (m/s^2)
Frequency (1/(Sec))

(k) **(l)**

Figure 4: Time and Frequency domain for the monitored grooved tube that is surrounded by rigid tubes in a parallel triangular arrangement with a P/D of 1.45 for (a, b, c, d) for 2nd row, (e, f, g, h) for 3rd row and (i, j, k, l) for 4th row at velocities 3.7, and 8.2 m/s.

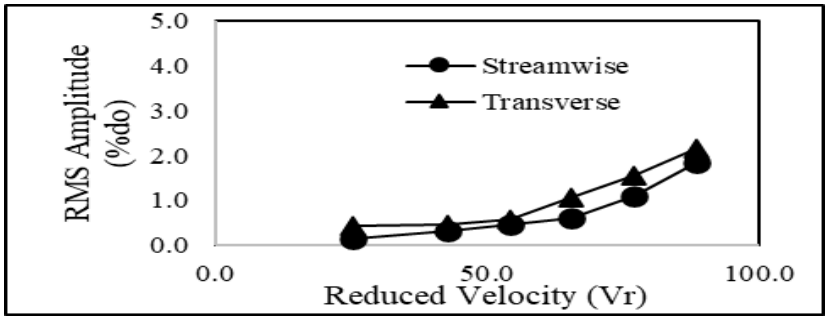

(a)

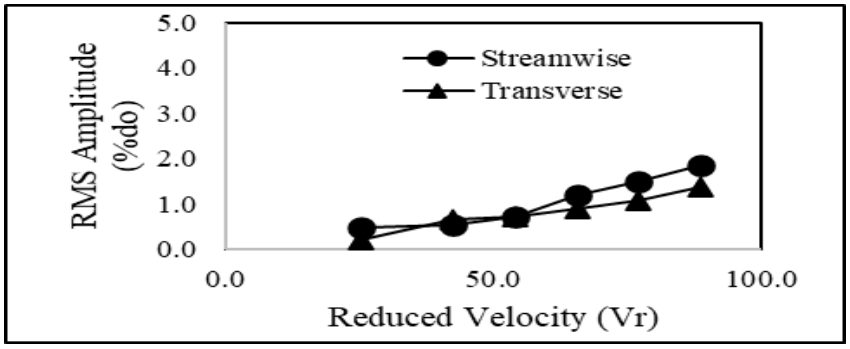

(b)

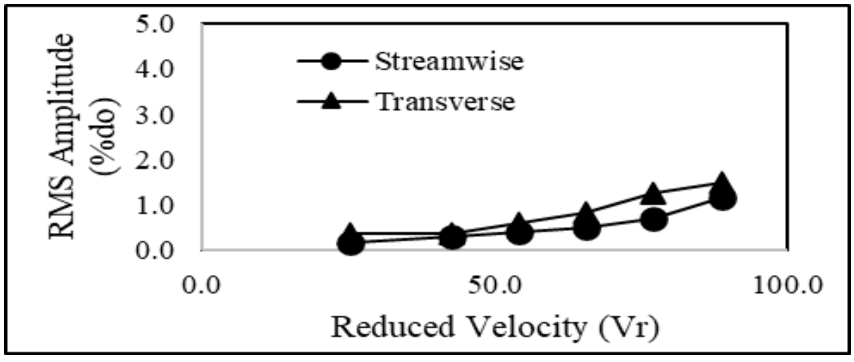

(c)

Figure 5: Stream-wise and transverse motion of the grooved tube at a P/D of 1.45 at different reduced velocity values or Amplitude response placing the tube in (a) Second row (b) Third row (c) Forth row

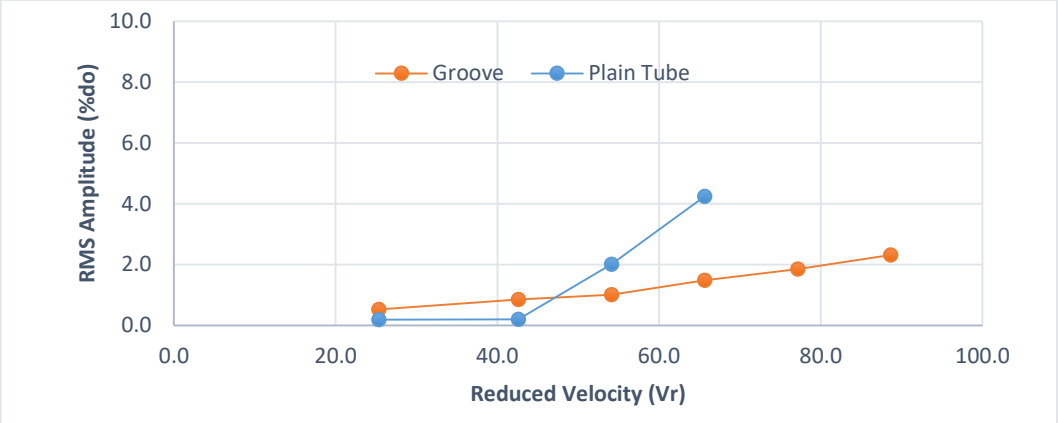

Figure 6: Comparison of results with publish results of plain tube [12]

4. Discussion

Frequency spectrum of 2nd row shows the increase in amplitude of the tube of about 0.05 at velocity of 3.7 m/s and 0.15 at a velocity of 8.2 m/s. Hence this sudden increase in amplitude by increasing flow velocity is responsible for the instability of the tube and results in the vibrations of the tube (Figure 4(b, d)). Frequency spectrum of 3rd row shows the increase in amplitude of the tube of about 0.24 at velocity of 3.7 m/s and 0.58 at a velocity of 8.2 m/s. Hence this sudden increase in the amplitude by increasing flow velocity is responsible for the instability of the tube and results in the vibrations of the tube. In the other rows, the amplitude is seen to be less than that of the 3rd row and showing the tube to be stable at the analyzed tube velocities (Figure 4(f, h)).

Frequency spectrum of 4th row shows the increase in amplitude of the tube of about 0.1 at velocity of 3.7 m/s and 0.09 at a velocity of 8.2 m/s. Hence this sudden increase in amplitude by increasing flow velocity is responsible for the instability of the tube and results in the vibrations of the tube (Figure 4(j, l)).

Instability appears to be characterized by a rapid increase in amplitude, which may be the result of the resonance phenomenon, which happens when the frequency of vibration is similar to the tube's inherent frequency. A similar trend can be seen in a third-row spectral analysis. So, it follows that the geometric characteristics of the tube and the degree of turbulence substantially affect the critical velocity of the fluid elastic vibration. The instability was pushed back in all the other rows, but the frequency response was changed somewhat upward because of the increased turbulence upstream. The translational mode appears to be suppressed by fluid coupling in the case of many flexible tube bundles.

Reduced velocity is a parameter used to study flow-induced vibrations, which measures the ratio between the flow velocity, the characteristic length of the vibrating structure, and

the natural frequency of the structure. This parameter helps predict if the flow-induced vibrations will occur in the system, and if the reduced velocity exceeds a critical value, the vibration may cause fatigue and failure of the structure over time. Fig. 5. depicts the transverse as well as stream-wise responses of the monitored grooved tube in a bundle of triangular tubes with a pitch to diameter ratio of 1.45 and subjected to cross-flow.

In the 2nd row of tube bundle, the stream-wise and the transverse amplitude of the grooved tube are slightly different from other. Transverse motion is more than the streamwise motion of the tube, instability is seen both stream-wise and transversely, as shown in Fig. 5(a). In the 3rd row of tube bundle, the stream-wise and the transverse amplitude of the grooved tube are slightly different from each other. Transverse motion is less than the streamwise motion of the tube resulting in less RMS amplitude percentage. When the monitored tube is positioned in the 3rd row of the tube bundle, instability is seen both stream-wise and transversely, as shown in Fig. 5(b). In the 4th row of tube bundle, the stream-wise and the transverse amplitude of the grooved tube are slightly different from each other. Transverse motion is more than the streamwise motion of the tube. So, when the monitored tube is positioned in the 4th row of the tube bundle, instability is seen both stream-wise and transversely, as shown in Fig. 5(c). The fourth row showed less instability compared to the other rows, with a maximum amplitude of 1.9% of the tube diameter and instability observed at a reduced velocity gap of approximately 80 in both the streamwise and transverse directions Fig. 5(c). Figure 6 shows that comparison of results by using plain tube, and grooved tube in tube bundle. RMS amplitude of the tube is decreased by using the grooved tube in the bundle instead of plain tube.

In summary, the response of monitored tube appears to be strongly influenced by its position inside a particular row in both the stream-wise and transverse directions. Additionally, the third row plays a crucial role in the early stability of the tube being monitored specifically in the transverse direction. As the RMS amplitude of the tube is decreased by using the grooved tube in the bundle instead of plain tube, the instability is reduced resulting in the increased life span of heat exchanger. So, the performance of heat exchanger is improved by using grooved tube instead of plain tube.

5. Conclusions

Experiments are conducted on turbulent cross-flow in a bundle of staggered tubes with a P/D of 1.45. The arrangement includes cylinders with grooves. The results obtained verified the previous theoretical and experimental data that is obtained using the same type of tubes.

It's crucial to conduct numerical and experimental studies to clarify the physical facts that the theory tries to explain. The monitored tube response appears to be strongly influenced by its position. Additionally, the third row plays an important role in the early stability of the tube being monitored specifically in the transverse direction. It can be concluded that the degree of turbulence as well as the geometric parameters of the tube have a great impact on the critical velocity of the fluid elastic instability. It is seen that the instability is further delayed in all other rows showing them to be more stable than the 3rd row. The performance of heat exchanger is improved by using grooved tube instead of plain tube.

Author Contributions: “Experimentation, Javaria Qadeer and Muhammad Moin Akhtar.; Literature, Hassan Shehwar Shah and Bushra Nadeem.; validation, Javaria Qadeer.; formal analysis, Javaria Qadeer.; writing—original draft preparation, Muhammad Moin Akhtar.; writing—review and editing, Riffat Asim Pasha.; supervision, Riffat Asim Pasha and Muhammad Ammar Akram.;”

Funding: This research received no external funding.

Acknowledgments: This research was accomplished under the supervision of Chairman Mechanical Engineering Department of UET Taxila.

Conflicts of Interest: The authors declare no conflict of interest.

References

[1] G. X. J. D. K. Z. M. Z. H. &. W. J. Zhao, "Numerical analysis of hydroenergy harvesting from vortex-induced vibrations of a cylinder with groove structures," Ocean Engineering, 2020.

[2] Y. Z. &. J. R. K. Law, "Passive control of vortex-induced vibration by spanwise grooves," Journal of Fluids and Structures, vol. 83, pp. 1-26, 2018.

[3] B. F. X. W. J. &. T. W. Tang, "Energy harvesting from flow-induced vibrations enhanced by meta-surface structure under elastic interference.," International Journal of Mechanical Sciences, 2022.

[4] L. K. &. D. L. Doreti, " Control techniques in flow past a cylinder-A Review.," materials science and engineering, vol. 1, 2018.

[5] S. Huang, "VIV suppression of a two-degree-of-freedom circular cylinder and drag reduction of a fixed circular cylinder by the use of helical grooves.," Journal of Fluids and Structures, vol. 27(7), pp. 1124-1133, 2011.

[6] Z. S. C. L. Y. B. K. &. Z. T. Hao, "Suppression of Vortex-Induced Vibration and Phase-Averaged Analysis of the Wake Generated by a Circular Cylinder Covered with Helical Grooves," Fluids, vol. 7(6), p. 194, 2022.

[7] J. F. &. G. N. Derakhshandeh, " Numerical investigations on the flow control over bumped surface circular cylinders.," Ocean Engineering, 2021.

[8] L. Z. Q. Z. L. &. W. H. Ding, "Research on flow-induced vibration and energy harvesting of three circular cylinders with roughness strips in tandem," Energies, vol. 11(11), 2018.

[9] J. F. &. G. N. Derakhshandeh, "Laminar flow instabilities of a grooved circular cylinder.," Journal of the Brazilian Society of Mechanical Sciences and Engineering, vol. 42(11), pp. 1-16, 2020.

[10] C. &. S. B. Canpolat, "Influence of single rectangular groove on the flow past a circular cylinder.," International Journal of Heat and Fluid Flow, vol. 64, pp. 79-88, 2017.

[11] J. F. T. Z. G. &. G. N. Derakhhsandeh, "Thermo-fluids effects of a grooved circular cylinder in laminar flow regimes," International Communications in Heat and Mass Transfer, vol. 124, 2021.

[12] Akram, M. A., Khushnood, S., Tariq, S. L., Nizam, L. A., & Ali, H. M. (2021). The effect of grid generated turbulence on the fluidelastic instability response in parallel triangular tube array. Annals of Nuclear Energy, 158, 108245.